

LiNH₂BH₃·NH₃BH₃: Structure and Hydrogen Storage Properties

Chengzhang Wu,[†] Guotao Wu,^{*,†} Zhitao Xiong,[†]
Xiuwen Han,[‡] Hailiang Chu,[†] Teng He,[†] and
Ping Chen^{*,†}

[†]Dalian Institute of Chemical Physics and [‡]State Key Laboratory of Catalysis, Dalian Institute of Chemical Physics, Chinese Academy of Sciences, Dalian 116023, China

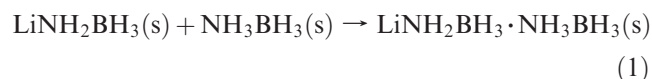
Received October 14, 2009

Revised Manuscript Received November 21, 2009

The development of a viable hydrogen storage system is of significant importance for the implementation of hydrogen fuel cell technology. Research efforts mainly focus on materials composed of light elements and with high hydrogen content.^{1–3} Ammonia borane (NH₃BH₃, AB for short), with 19.6 wt % hydrogen capacity, has attracted considerable attention recently.^{4–17} However, the thermal decomposition of neat AB occurs at relatively high temperature (100 °C and above) and gives volatile byproducts, such as aminoborane and borazine.⁴ In the past several years, a few approaches including the uses of transition metal⁵ or acid catalysts,⁶ hexagonal boron nitride,⁷ nanoscaffolds⁸ and carbon cryogels,⁹ and hydrolysis,^{10,11} and so forth, have been employed to improve the dehydrogenation performance of this substance. More recently, efforts have been given to the chemical

modification of AB through replacing one of its H with alkali or alkali earth element to form metal amido-borane (MAB).^{12–17} Xiong et al.¹² reported that alkali-metal amidoboranes, such as LiNH₂BH₃ (LiAB) and NaNH₂BH₃ (NaAB) crystallizing in orthorhombic space group *Pbca*, release large amount of hydrogen (10.9 wt % for LiNH₂BH₃ and 7.5 wt % for NaNH₂BH₃) without borazine formation at 91 °C. Alkali earth metal amido-borane, that is, Ca(NH₂BH₃)₂ (CaAB) synthesized by Diyabalanage et al.¹³ via wet-chemical route and Wu et al.¹⁵ via mechanical ball milling of CaH₂ and AB, dehydrogenates at temperatures above ~120 °C and gives ~4 equiv of H₂ upon heated to 250 °C.¹³ Apart from the variation in the dehydrogenation properties, the replacement of one H by alkali or alkali earth in AB leads to the transfer of molecular crystal (AB) stabilized by dihydrogen bond to ionic crystal (MAB).^{12,15} In this study, a new AB derivative, namely lithium amidoborane-ammonia borane in a chemical composition of LiNH₂BH₃·NH₃BH₃ (LiAB·AB for short) was synthesized by reacting equiv LiAB and AB or reacting LiH and 2 equiv of AB. LiAB·AB is composed of alternative layers of LiAB and AB and contains both dihydrogen bond and ionic bond in the crystal lattice. Experimental results show that this new compound releases 14.0 wt % of hydrogen in a stepwise manner with peak temperatures at ca. 80 and 140 °C, respectively. Borazine and aminoborane are undetectable.

A gradual H₂ pressure increase in the milling vial was observed when ball milling LiH and NH₃BH₃ mixture in a LiH/AB molar ratio of 1:2.¹⁸ Calculated from the pressure increase, the amount of H₂ evolved was about 1.0 equiv per mol of LiH upon the completion of reaction. In contrast, ball milling LiNH₂BH₃ and NH₃BH₃ in 1:1 molar ratio did not come out with any detectable gaseous product. X-ray powder diffraction measurements on the fresh samples collected immediately after ball-milling show that the patterns of the postmilled LiH-2AB and LiAB-AB samples are similar and present a new set of diffractions. Starting chemicals were undetectable (see Figure S1 in the Supporting Information). The information gathered above suggests that LiNH₂BH₃·NH₃BH₃ (or LiAB·AB) is formed through the reactions 1 and 2.



(18) NH₃ concentration in the gaseous product varies from below 100 ppm to a few thousand ppm depending on the quality of LiAB·AB sample, conditions in the sample preparation (temperature for the preparation, purities of reactants, etc.), and the conditions applied in the dehydrogenation (temperature, pressure, etc.). Our preliminary results showed that NH₃ is likely to be an intermediate in the dehydrogenation. Further investigation is undergoing.

*Corresponding authors. Email: wgt@dicp.ac.cn; pchen@dicp.ac.cn.

- (1) Chen, P.; Zhu, M. *Mater. Today* 2008, 11, 36.
- (2) Stephens, F. H.; Pons, V.; Baker, R. T. *Dalton Trans.* 2007, 25, 2613.
- (3) Orimo, S. I.; Nakamori, Y.; Eliseo, J. R.; Zuttel, A.; Jensen, C. M. *Chem. Rev.* 2007, 107, 4111.
- (4) Baitalow, F.; Baumann, J.; Wolf, G.; Jaenicke-Rossler, K.; Leitner, G. *Thermochim. Acta* 2002, 391, 159.
- (5) Clark, T. J.; Manners, I. J. *Organomet. Chem.* 2007, 692, 2849.
- (6) Stephens, F. H.; Baker, R. T.; Matus, M. H.; Grant, D. J.; Dixon, D. A. *Angew. Chem., Int. Ed.* 2007, 46, 746.
- (7) Neiner, D.; Karkamkar, A.; Linehan, J. C.; Arey, B.; Autrey, T.; Kauzlarich, S. M. *J. Phys. Chem. C* 2009, 113, 1098.
- (8) Gutowska, A.; Li, L. Y.; Shin, Y. S.; Wang, C. M. M.; Li, X. H. S.; Linehan, J. C.; Smith, R. S.; Kay, B. D.; Schmid, B.; Shaw, W.; Gutowski, M.; Autrey, T. *Angew. Chem., Int. Ed.* 2005, 44, 3578.
- (9) Feaver, A.; Sepehri, S.; Shamberger, P.; Stowe, A.; Autrey, T.; Cao, G. Z. *J. Phys. Chem. B* 2007, 111, 7469.
- (10) Kalidindi, S. B.; Indirani, M.; Jagirdar, B. R. *Inorg. Chem.* 2008, 47, 7424.
- (11) Xu, Q.; Chandra, M. *J. Power Sources* 2006, 163, 364.
- (12) Xiong, Z. T.; Yong, C. K.; Wu, G. T.; Chen, P.; Shaw, W.; Karkamkar, A.; Autrey, T.; Jones, M. O.; Johnson, S. R.; Edwards, P. P.; David, W. I. F. *Nat. Mater.* 2008, 7, 138.
- (13) Diyabalanage, H. V. K.; Shrestha, R. P.; Semelsberger, T. A.; Scott, B. L.; Bowden, M. E.; Davis, B. L.; Burrell, A. K. *Angew. Chem., Int. Ed.* 2007, 46, 8995.
- (14) Xiong, Z. T.; Wu, G. T.; Chua, Y. S.; Hu, J. J.; He, T.; Xu, W. L.; Chen, P. *Energy Environ. Sci.* 2008, 1, 360.
- (15) Wu, H.; Zhou, W.; Yildirim, T. *J. Am. Chem. Soc.* 2008, 130, 14834.
- (16) Kang, X. D.; Fang, Z. Z.; Kong, L. Y.; Cheng, H. M.; Yao, X. D.; Lu, G. Q.; Wang, P. *Adv. Mater.* 2008, 20, 2756.
- (17) Ramzan, M.; Silvearv, F.; Blomqvist, A.; Scheicher, R. H.; Lebegue, S.; Ahuja, R. *Phys. Rev. B* 2009, 79, 132102.

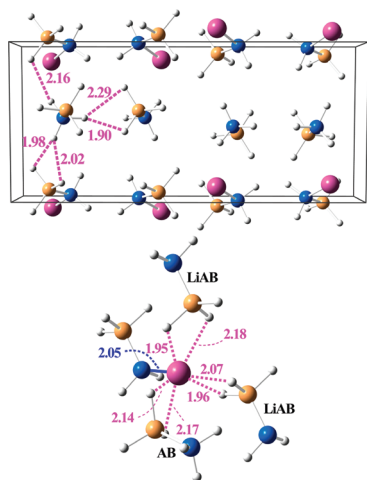
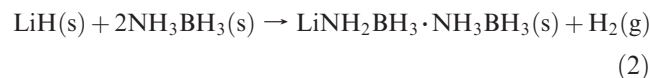


Figure 1. (Top) Schematic diagram of the crystal structure of LiAB·AB at room temperature. Li, B, N and H atoms are represented by purple, brown, blue and gray spheres, respectively. (Bottom) Coordination environment of Li^+ . Each Li^+ is directly bonded with one $[\text{NH}_2\text{BH}_3]^-$ ion and also coordinated with H atoms in $-\text{BH}_3$ group of one NH_2BH_3 and two LiNH_2BH_3 .



^{11}B NMR measurements show that BH_3 groups in LiAB·AB have two chemical environments, that is, at $\delta = -20.9$ and -26.5 ppm, close to that in LiAB ($\delta = -22$ ppm) and AB ($\delta = -26.2$ ppm),¹⁶ respectively (see Figure S2 in Supporting Information). The diffraction pattern of the compound recorded on high resolution synchrotron radiation XRD (SR-XRD) can be indexed using a monoclinic space group $P21/c$ cell with $a = 7.0536(9)$ Å, $b = 14.8127(20)$ Å, $c = 5.1315(7)$ Å, $\beta = 97.491(5)^\circ$, and $V = 531.58(12)$ Å³ (see Figure S1 in Supporting Information). Since the powder SR-XRD is of low sensitivity to H atom, it is necessary to use first-principles calculations to identify the atomic positions in the structure. The crystal structure of this new compound was then solved using the combined direct space simulated annealing method and first-principles calculations (see method in Supporting Information). The calculated lattice constants, that is, $a = 6.83065$ Å, $b = 15.10986$ Å, $c = 5.19075$ Å, $\beta = 97.0638^\circ$, and $V = 531.7$ Å³, are in consistent with the experimental data. As shown in Figure 1, the structure model of LiAB·AB is composed of alternative LiAB and AB layers, which agrees well with the NMR observations of two $-\text{BH}_3$ species resembling to LiAB and AB. Each Li^+ bonds with one $[\text{NH}_2\text{BH}_3]^-$ ion and is also coordinated with H atoms in BH_3 groups of AB and LiAB nearby with the Li–H distance in the range of 1.953–2.165 Å. Such a Li–H coordination will likely lead to the weakened dihydrogen bond in the AB layer. In fact, the distance between $\text{NH} \cdots \text{HB}$ (1.902 Å) in AB layer is a little longer than that in pristine AB (1.897 Å) (Supporting Information, Table S1).^{15,19} As the

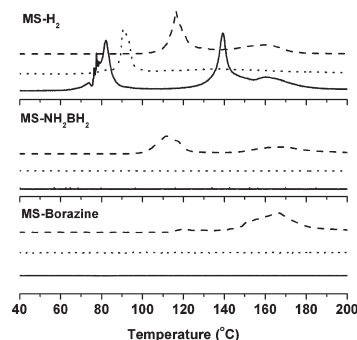


Figure 2. Thermal desorption mass spectra of LiAB·AB (solid line), LiAB (dotted line) and pristine AB (dashed line). The heating rate is 2 °C/min. There are borazine ($m/z = 81$) and aminoborane ($m/z = 29$) detected in the gaseous phase of AB. Slight amount of ammonia was also detected in all three samples.¹⁸

dihydrogen bond is one of the main components in stabilizing the crystal of LiAB·AB, the lattice of LiAB·AB, may be subject to deform comparatively easily. Our DSC measurements show that the onset melting temperature of LiAB·AB is 58 °C, considerably lower than that of LiAB (82 °C) and AB (95 °C) (Figure S3, Supporting Information).

In a previous investigation on the interaction of LiH and AB at varied molar ratio, the formation of LiAB·AB ($Cmc2_1$ cell, with $a = 13.992$ Å, $b = 10.742$ Å, and $c = 10.110$ Å) was proposed when ball milling LiH with 2 equiv of AB.¹⁵ It should be noted that the structure determined by us is significantly different from that structure reported previously. Our experimental observations reveal that LiAB·AB decomposes slowly at temperatures above 25 °C. The diffraction peaks of self-decomposed sample (Figure S4, Supporting Information, there are three main diffraction peaks at $2\theta = 10.3^\circ$, $2\theta = 22.7^\circ$, and $2\theta = 31.4^\circ$) can be found in the LiAB·AB pattern reported¹⁵ and also resembles to the α -phase described in a published patent.²⁰

Thermal desorption mass spectrometer (TDMS) profiles of the LiAB·AB, LiAB, and pristine AB samples are shown in Figure 2. LiAB·AB decomposes exothermically to hydrogen in a stepwise manner with peak temperatures at ~ 80 °C and ~ 140 °C, respectively. In addition, a relatively weak desorption appears at ~ 160 °C. The overall feature exhibits remarkable differences from those of LiAB and neat AB in that the first desorption peak appears at lower temperature (80 °C vs ca. 91 °C for LiAB and ca. 110 °C for AB) and the sum of peak areas of the second and third peaks is larger than that of the first peak showing more hydrogen desorption at higher temperatures. Moreover, aminoborane and borazine are undetectable. We tentatively ascribe the lowered dehydrogenation temperature to the reduced melting point of LiAB·AB. Moreover, the dehydrogenation of LiAB or AB is likely through intermolecular interaction.^{12,21}

(19) Lee, S. M.; Kang, X. D.; Wang, P.; Cheng, H. M.; Lee, Y. H. *ChemPhysChem* **2009**, *10*, 1825.

(20) Torgersen, A. N.; Jorgensen, S. W. US20060097221 A1, Oct. 28, 2005.

(21) Kim, D. Y.; Singh, N. J.; Lee, H. M.; Kim, K. S. *Chem.—Eur. J.* **2009**, *15*, 5598.

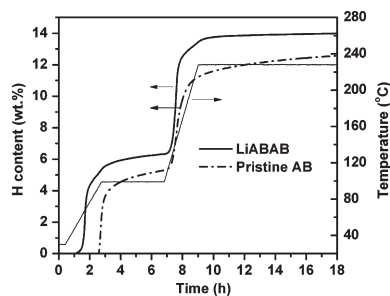
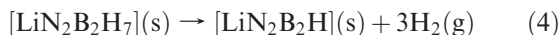
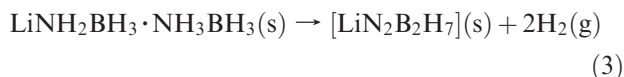


Figure 3. Time dependence of hydrogen desorption from LiAB·AB and pristine AB. Both samples were first heated to 100 °C at a ramping rate of 0.5 °C/min and kept at 100 °C for 4 h, then further heated to 228 °C and kept for 10 h.

The chance of reaction will be considerably enhanced when reacting molecular species are mobile.

To quantitatively measure hydrogen desorption from LiAB·AB, a volumetric release test was performed at 100 and 228 °C, respectively. As shown in Figure 3, LiAB·AB starts to release hydrogen at 57 °C, ca. 6.0 wt % or 2 equiv of H₂ is released in the first step.¹⁸ Further increasing temperature to 228 °C leads to the release of additional ca. 8.0 wt % or about 2.7 equiv of H₂. Therefore, nearly 5 equiv of H₂ can be released from LiAB·AB at 228 °C. In both steps, LiAB·AB releases more hydrogen at faster rates than pristine AB. It is important to note that there are maximum 4 equiv of “releasable” H atoms in LiAB,¹² so that nearly all hydrogen (ca. 6 equiv. Hs) of AB in LiAB·AB can be detached in the temperature range of 50 to 228 °C, which is significantly lower than the temperature required to release the same amount of H₂ from neat AB (above 500 °C).²² The compositional change in the material, that is, replacing 1/6 of H bonded with N by Li, induces significant variations in the thermodynamic and kinetic properties of AB. Simulation work on the dehydrogenation of LiAB revealed that the removal of H from –BH₃ is through a transition state where that H bents over to Li nearby and establishes a H–Li bond. In other words, the presence of Li creates an energy favored pathway in the dehydrogenation.²¹ The enhanced hydrogen desorption in LiAB·AB should also own to the presence of Li in the system. More detailed investigation is needed. As ca. 2 and ca. 3 equiv of H₂ desorbed in the lower (50–100 °C) and higher (120–228 °C) temperature ranges, respectively, the reactions 3 and 4 can be used to describe this stepwise dehydrogenation. H may be detached from LiAB and AB layers simultaneously in the first step.



XRD characterizations reveal that [LiN₂B₂H₇] exhibits identical pattern as that of the self-decomposed

LiAB·AB (Figure S4, Supporting Information), while [LiN₂B₂H] is amorphous in nature. From stoichiometric point of view, [LiN₂B₂H₇] may be LiNHBH₂·NH₂BH₂ or LiNH₂BH=NHBH₃. NMR characterizations show that B species at $\delta = -24.1$ ppm and at around $\delta = 20$ ppm were present in [LiN₂B₂H₇] (Figure S5, Supporting Information), which resembles to that of raw polyamino-borane (PAB) reported by Kim et al.²³ and Gervais et al.,²⁴ showing the likelihood of the formation of PAB-like product, i.e., LiNHBH₂·NH₂BH₂. However, we can not rule out the existence of LiNH₂BH=NHBH₃ because the signals at –24 and 20 ppm can also be assigned to the terminal –BH₃ and the sp² –BH species, respectively. Detailed structural investigation is necessary. After dehydrogenated to 228 °C, the sample possesses stronger resonance centered at ca. 20 ppm. A –BH₄ species at ca. –40 ppm appears which is probably due to the formation of minor LiBH₄. Noted that –BH₄ resonance is very weak in the first step (see Figure S5, Supporting Information), the majority of the species should be formed in the follow-up dehydrogenation at higher temperatures. Similar phenomenon was also observed in the solid-state dehydrogenation of LiAB to elevated temperatures.¹¹ To clarify this, ¹H → ¹¹B cross-polarization was performed on the postdehydrogenated (to 228 °C) sample. As shown in the Figure S5 (Supporting Information), B species having chemical shift in the range of 10–40 ppm carries little hydrogen, while the majority of hydrogen is bonded by B at –41 ppm. We suggest that [LiN₂B₂H] is made of BN, Li₃BN₂ and LiBH₄ according to 4[LiN₂B₂H](s) → Li₃BN₂(s) + 6BN(s) + LiBH₄(s). LiBH₄, BN and Li₃BN₂ can hardly crystallize under the dehydrogenation condition, so that little information was obtained from the XRD characterization. Further investigation is needed.

In summary, a new AB derivative, namely lithium amidoborane–ammonia borane, has been synthesized successfully. The release of 14.0 wt % of hydrogen at reduced temperatures from LiAB·AB enables it to be a promising candidate for hydrogen storage. Further investigations are needed to understand the reaction mechanism and to enhance the dehydrogenation kinetics.

Acknowledgment. The authors acknowledge the financial support from the Hundred Talents Project and Knowledge Innovation Program of CAS (KGCX2-YW-806 and KJCX2-YW-H21), 863 project (2009AA05Z108) and 973 Project (2010CB631304). The structural identification was performed at BL14B1 of Shanghai Synchrotron Radiation Facility (SSRF). The authors are also grateful for beneficial discussions with IPHE collaborators including Bill David (ISIS, RAL) and Martin Jones (Oxford) and assistance from Dr. Wen Wen (SSRF).

Supporting Information Available: Experimental section and additional figures (PDF). This material is available free of charge via the Internet at <http://pubs.acs.org>.

(22) Hu, M. G.; Geanangel, R. A.; Wendlandt, W. W. *Thermochim. Acta* **1978**, 23, 249.

(23) Kim, D. P.; Moon, K. T.; Kho, J. G.; Economy, J.; Gervais, C.; Babonneau, F. *Polym. Adv. Technol.* **1999**, 10, 702.

(24) Gervais, C.; Babonneau, F. *J. Organomet. Chem.* **2002**, 657, 75.